Journal of Equine Veterinary Science 121 (2023) 104206

Contents lists available at ScienceDirect

Journal of Equine Veterinary Science

journal homepage: www.j-evs.com

Review Article

An Overview of Factors Affecting Exposure Level in Digital Detector Systems and their Relevance in Constructing Exposure Tables in Equine Digital Radiography

Eberhard Ludewig*, Conor Rowan, Katrin Schieder, Ben Frank

Diagnostic Imaging, Department of Small Animals and Horses, University of Veterinary Medicine Vienna, Vienna, Austria

ARTICLE INFO

Article history:
Received 6 March 2022
Received in revised form 23 December 2022
Accepted 26 December 2022
Available online 6 January 2023

Key words:
Digital radiology
Exposure table
Exposure indicator
Image quality
Detector quantum efficiency
DQE

ABSTRACT

The aim of this review is to describe the steps of constructing exposure tables for use of digital detector systems (DRx) in equine practice. Introductory, selected underlying technical aspects of digital radiography are illustrated.

Unlike screen-film radiography (SFR), DRx have a uniform signal response of the detector over a large dose range. This enables generation of diagnostic images from exposures that were previously nondiagnostic on SFR, thus reducing retakes. However, with decreasing detector entrance dose, image noise increasingly hampers the image quality. Conversely, unlike the blackening observed on SFR, overexposures can go visibly undetected by the observer. In DRx the numeric exposure indicator value is the only dose-control tool. In digital radiography the challenge is to reduce the dose and reduce the radiation risk to staff whilst maintaining diagnostic image quality. We provide a stepwise method of developing exposure tables as tools for controlling exposure levels. The identified kVp - mAs combinations in the table are derived from the predefined exposure indicator values of the detector system. Further recommendations are given as to how the exposure indicator can be integrated into routine workflow for rechecking the reliability of the formerly identified settings and how these tables might serve a basis for further reduction of the exposure level. Detector quantum efficiency (DQE) is an important parameter of assessing performance of an imaging system. Detectors with higher DQE can generate diagnostic images with a lower dose, thus having a greater potential for dose reduction than detectors with low DQE.

1. Introduction

In veterinary radiology, digital detector systems (DRx) have largely replaced screen-film systems. In a survey in 2013, 75% of small animal practices were using digital radiographs in the UK and Ireland [1]. In Ireland, meanwhile all equine practitioners have replaced screen film radiography (SFR) with DRx [2]. One can only assume this trend has continued and is mirrored in other countries.

Two significant advantages are driving this adoption of new technology in equine practice. DRx - in particular flat-panel detectors - can easily be integrated into the technical infrastructure of a mobile practice and can achieve a constantly high image quality [3,4]. DRx emit a uniform signal over a broad dose range. On the one hand, this enables DRx to forgive exposure faults avoiding retakes of images for this reason. On the other hand, overexposures are not readily visible. Unlike SFR, image brightness is completely independent from exposure settings in digital radiography [5–7].

In contrast to human radiology - where it is mandatory to establish alternative tools of exposure control and monitoring primarily for patient protection [6] - comparable precise and legally binding obligations for veterinary applications do not exist in Europe to our knowledge. The application of suitable tools is relevant in veterinary radiology so as to avoid unnecessary radiation exposures of both staff and animal patients [8,9].

This article first provides an overview of technical terms and principles of digital radiography as related to exposure level and image quality. In the second part, we demonstrate the principle of developing exposure tables for equine radiography and how the system-specific exposure indicator can subsequently be integrated into the clinical routine for ongoing tracking of the exposure level.

Conflict of interest statement: The authors declare no conflict of interest.

Animal welfare/ethical statement: Authors have adhered to ethical guidelines outlined in https: //www.elsevier.com/authors/journal-authors/policies-and-ethics.

* Corresponding author at: Eberhard Ludewig, Diagnostic Imaging, Department of Small Animals and Horses, University of Veterinary Medicine Vienna, Veterinärplatz 1, Vienna, 1210, Austria.

https://doi.org/10.1016/j.jevs.2022.104206

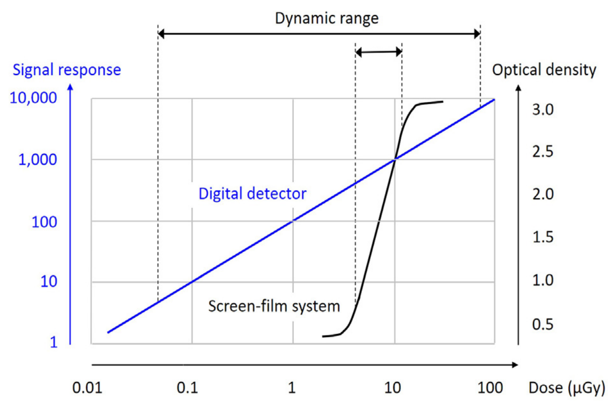

Fig. 1. Characteristic curve. The scheme illustrates the dynamic range of DRx and SFR. In contrast to SFR, DRx cover a very wide exposure range (adapted from [11]).

The described approach can serve as a guidance to support optimization of exposure technique in veterinary practice.

2. Physical Principles of Digital Radiography

2.1. 'Characteristic Curve' and 'Dynamic Range'

'Characteristic curve' ('intensity transfer function') is a graph describing the relationship between the detector entrance dose and the signal response of the detector [10,11]. In SFR, 'signal' is equivalent with 'optical density' which again is a physical measure of the blackening of the film. The curve is steep and sigmoid-shaped. 'Dynamic range' defines the range of X-ray attenuation differences detectable. In SFR it is low and correlates with narrow exposure limits. As soon as the detector entrance dose is outside of these limits, the image is either underexposed (too bright = too low optical density) or overexposed (too dark = to high optical density). Consequently, film blackening is a very useful direct indicator about the detector entrance dose [10,12]. In contrast, DRx are able to register signal differences in a linear manner over a very wide exposure range. The dynamic range of DRx exceeds more than 100 times the range of SFR [10,11] (Fig. 1).

From these technical characteristics, a number of consequences for the use of DRx can be derived:

- Digital radiography overcomes the dynamic range limitations of SFR. The dynamic range of digital systems range from 10 (1,024 shades of gray) to 16 bit (65,536 shades of gray). The large number of gray scales represents superior image contrast [6,11].
- In digital radiography image brightness is not related with the detector entrance dose. Instead, gray scale displaying is entirely determined by the algorithm of signal processing and the mapping of the individual pixel values into monitor signal by predefined translation regulations, so-called 'look-up tables' (LUT) [13,14]. Because brightness is not usable for the visual exposure control, there is an obvious risk for undetected ongoing overexposures [15,16].
- The large dynamic range allows potential dose reduction. However, with decreasing detector entrance dose image noise - pixelation of the images best seen in areas of the image with uniform X-ray attenuation - is getting increasingly obvious [13,17,18]. A decreasing 'signal-to noise ratio' (SNR) means that the level of the given background noise originating from the detector cannot be compensated by a sufficient number of X-ray photons (Fig. 2). Therefore, the question arises at which point of dose reduction is the noise significantly obscuring image details and thus unacceptably limits the diagnostic value of the image. The question is not easily answered because the 'beauty of an image' has to be distinguished from the 'diagnostic suitability of an image'. In particular, the latter represents a category that is based on very subjective assessments [19].
- Higher detector exposures produce images with improved noise characteristics. But this is at the expense of increased staff and animal patient doses resulting in increased stochastic radiation risks. The phenomenon of ongoing up-ward exposure adjustments to be 'on the safe side' with regard to image quality is called 'dose creep' [20,21].
- Extreme mal-exposures visibly hamper image quality. Extreme overexposure results in detector saturation in which the ability of the detector to record low attenuation differences in low attenuating body parts got lost. Extremely underexposed images cannot be evaluated because of low SNR-based pixilation [6,8,13] (Fig. 2). The described signal characteristics and technical interrelationships underline the need to implement robust and easily applicable exposure monitoring tools for veterinary radiography. The twin objectives are clear: protecting people carrying out examinations and animal patients from unjustified, high doses whilst maintaining a diagnostic image quality.

Table 1
Exposure indicators. The factors listed influence histogram analysis. Errors in the histogram analysis lead to incorrect exposure indicator values.

Factor	Cause
Exposure field recognition error	Collimation margins not correctly detected • object placed outside the center of the exposed field • very small objects • very small field-size • failure of the analysis software to detect margins of the exposed field
Metallic materials	Histogram widening due to unusual pixel values
Extreme overexposure	Histogram widening due to unusual pixel values
Extreme underexposure	Histogram analysis error due to excessive quantum mottle

2.2. Exposure Indicators

In digital radiography, a useful tool for the identification of the achieved level of exposure is to review the value of the exposure indicator provided by the imaging system. These exposure indicators do not result from any dose measurement. Instead, exposure indicators are numerical parameters derived from the recorded signal characteristics. The parameter is calculated from the conversion of the pixel values during the exposure. Pixel values represent the intensity of light photons deposited in the pixel. The radiation level at the surface of the detector can be derived from the frequency and distribution of these pixel values ('histogram') [6]. The value represents a relative exposure measure and correlates with the achieved SNR [22]. Therefore, the displayed values of the exposure indicator can be used twofold, as a tool to track the detector entrance dose and as a tool to control noise-based image quality [23–25] (Fig. 3).

It has to be taken into account that several factors others than the detector entrance dose influence the exposure indicator value. Significant fluctuations of the display values arise from differences of the collimation, changes of the processing algorithms and errors in the histogram analysis [6,26] (Table 1). Therefore, it is important to avoid such errors by standardization of the acquisition technique and, if unavoidable, respect these factors while interpreting exposure indicator values.

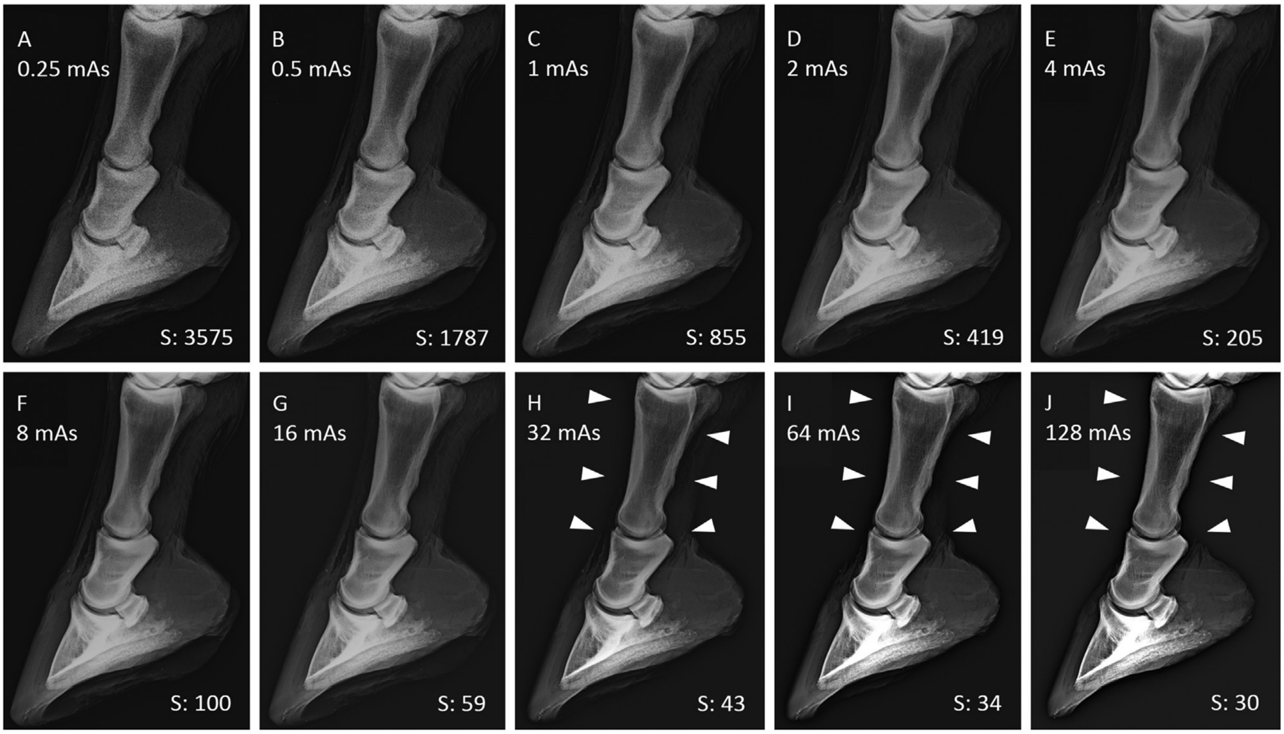

Fig. 2. Effects of the detector dose on the quality of digital images. The images of a cadaver limb are labeled with mAs settings and corresponding S-values. All images were obtained with a flat-panel detector (FDR D-EVO II C24i, Fujifilm Corporation, Tokyo, Japan) at 60 kVp and uniform focus-detector distance, collimation and processing parameters. Due to use of an adaptive LUT, differences in brightness and contrast are compensated. Over a wide dose range there are no visible differences of the image quality. Exclusively extremely low doses (A) attribute to a significant noise-based blurring of anatomic structures. At very high doses (H–J) soft tissues are increasingly obliterated ('burnt out') from the radiograph due to detector saturation (arrowheads).

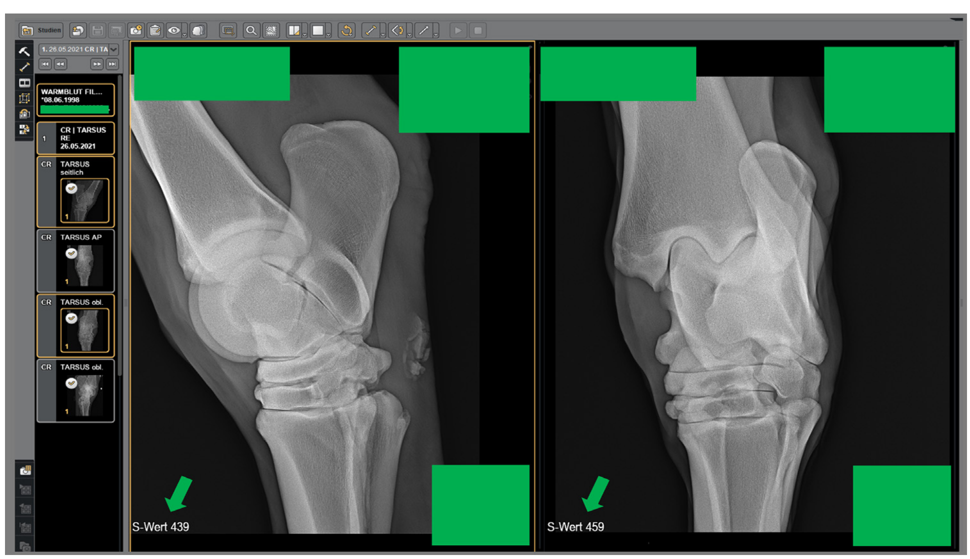

Fig. 3. Screenshot of a workstation monitor. The value of the exposure indicator - here the S-value (green arrow) - is displayed as part of the image information.

With the introduction of the first digital detector system in the 1980s the individual manufacturers established their own proprietary exposure indicators. Over time, the multitude of existing parameters with different scaling of the values made comparisons difficult. Thankfully, manufacturers are increasingly adopting the unified 'standardized exposure index' (S-EI)(Table 2). This standard was defined by the International Electrotechnical Commission (IEC 62494-1) [27] and the American Association of Physicists in Medicine (AAPM tg-116) [28] to overcome the difficulties related with the use of the diverse existing indicators. S-EI is independent of the manufacturer and the technology. Meanwhile, it has proven to be overall reliable in human radiology [29,30] and it was demonstrated that even patient doses could be estimated from the generated data [31,32].

The advantage of S-EI is that the user only had to be familiar with the meaning of three parameters:

1 'Exposure index' (EI) is the value displayed for an individual image. The value is a function of the applied exposure settings (kVp, mAs), but also of the predefined examination type

Table 2
Exposure indicators. Relationships between detector doses, the standardized exposure index (S-EI) values and proprietary reporting terminology of selected manufacturers. Due to differences in calibration the presented data demonstrate approximate relationships (compiled from [6,23,43,53].

Detector Dose (μGy)	Parameter	1.25	2.5	5	10
IEC, AAPM	EI (S - EI)	125	250	500	1,000
Agfa (SC 200)	lgM	1.3	1.6	1.9	2.2
Agfa (SC 400)	lgM	1.6	1.9	2.2	2.5
Canon (B 16, C 10)	REX	12.5	25	50	100
Carestream (CR, STD)	EI	1,100	1,400	1,700	2,000
Fuji, Konica	S	1,600	800	400	200
Philips	EI	800	400	200	100
Siemens	EXI	190	380	760	1,520

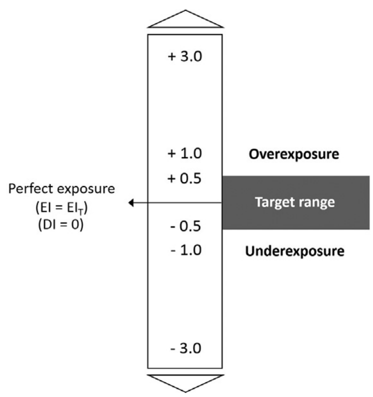

Fig. 4. Standardized exposure index (S-EI). Range of DI values and the AAPM recommendations on the interpretation for clinical use in human radiology. The target range is 0 ± 0.5. For DI from +1 to +3 ('overexposure') and greater than +3 (excessive radiation exposure) from the image quality point of view the action is 'repeat only if necessary'. Basically, this is the same for values lower than −1 (underexposed). Mostly images with DI lower than -3 are nondiagnostic and must be repeated. From the radiation safety point of view, values outside the target range require immediate efforts to prevent further exposure faults (adapted from [28]).

(e.g., hoof, carpus) and the 'region of interest (ROI)' identified in the signal processing. EI is linearly related to detector exposure. Therefore, for example, doubling the mAs settings doubles the EI.

2 'Target EI' (EI_T) is the reference for an optimal exposure. It could be defined either by the manufacturer giving recommendations based on image receptor dose for certain applications or by the veterinary user. The latter preferably should be based on results of image quality studies.

3 The 'deviation index' (DI) quantifies the degree of deviation of the actual EI from the EI_T. In an ideal scenario, it should be zero, that is, EI and EI_T are the same. DI is calculated from $DI = 10\log_{10}(EI/EI_T)$. Deviations of exposure settings from the predefined level are easy to recognize. The AAPM has made suggestions on the interpretation of DI-values for clinical use in human radiology. The tolerable range for the DI-value is 0 ± 0.5. As it is a logarithmic scale; a DI-value of +3 indicate that EI is twice the EI_T, and a DI value of -3 means that EI is half of EI_T [28] (Fig. 4). For veterinary radiology these recommendations may serve as a starting point for further adjustments.

For digital radiography systems where the S-EI is not available, the feasibility of adding this capability (e.g., with a software upgrade), should be explored. The uniform use of S-EI can give better control and make users less susceptible to misinterpretation of recorded data, especially in departments equipped with multiple digital systems from differing manufacturers.

Regardless of the type of exposure indicator that is implemented in a given imaging system; dose indicators are an easily applicable method of monitoring the exposure level, providing a good orientation. The approach is always the same: Each examination has a predefined target exposure indicator range that the real value is compared with. Values outside this tolerable range indicate too high or too low detector entrance doses. Monitoring of the displayed value can thus be easily integrated into the routine workflow (Fig. 3).

Table 3
Selected technical features of digital imaging systems. In contrast to minor differences in the pixel size, remarkable differences of the detective quantum efficiency (DQE) exist between the systems.

Computed Radiography
Pixel size: 100 ... 200 μm (5 ... 2.5 lp mm^{-1})
CR with powder-structured image-plate
X-ray recording: $BaFX:Eu^{2+}$ photostimulable phosphor
DQE (70 kVp, 1 lp mm^{-1}): 18 ... 25 %
Dual-side reading CR
X-ray recording: BaFBrl:Eu2+ photostimulable phosp1hor
DQE (70 kVp, 1 lp mm^{-1}): 30 %
CR with needle-structured image-plate
X-ray recording: CsBr:Eu2+ photostimulable phosphor
DQE (70 kVp, 1 lp mm^{-1}): 35 %
Flat panel detectors
Detector element size: 100 ... 200 μm (5 ... 2.5 lp mm^{-1})
Indirect conversion
X-ray recording: Gd_2O_2S or CsI phosphor + TFT array
DQE (70 kVp, 1 lp mm^{-1}): 50 / 65 %
Direct conversion
X-ray recording: amorphous Se photoconductor + TFT array
DQE (70 kVp, 1 lp mm^{-1}): 30 %

2.3. Detector Technologies

Two different detector technologies are currently in use (overviews in [6,11,33,34] (Table 3).

2.3.1. Computed Radiography (CR) (Synonym: Storage Phosphor System)

In CR-systems, introduced in the mid-1980s, a cassette contains a storage-phosphor plate. The plate has a layer of photostimulable crystals with halogenides, representing the sensor material. During the readout process - performed by a separate reader unit - laser light is applied to release the stored energy. Photodiodes then capture the emitted visible light and convert it into a digital signal. Depending on the plate size and the scan matrix, the readout process takes approximately 20 to 40 seconds.

Since its introduction, the modification of the basic CR principle has improved readout speed, spatial resolution and sensitivity. If the use of a CR system in mobile equine practice is planned, it should be noted that the readout unit needs some space in the car, and that it is less tolerant for mechanical vibrations, dust and fluctuations of temperature and humidity.

2.3.2. Flat-Panel Detectors (Synonyms: Direct Radiography, DR; Direct Digital Radiography, DDR)

Flat-panel detectors convert X-rays direct into electrical charge without intermediate mechanical read-out steps. Image is immediately available.

Since 2000, two subtypes of flat-panel detectors are in use:

- Indirect flat-panel detectors has an upper scintillator layer (cesium iodide, gadolinium- or lanthanum oxide sulfide) where X-rays are converted into visible light. Underneath the scintillator, there is an array of semiconductors of amorphous silicon (a-Si). Each pixel contains a photodiode, a capacitor and a thin-film transistor (TFT). The photodiode converts the incoming light into electrons. The capacitor stores this electric charge

Table 4
Technical features of the detector (data from Fujifilm, Tokyo, Japan: https://www.fujifilm.com).

Feature	Specification - Data
Flat-panel detector	FDR D-EVO II C24i
Manufacturer	Fujifilm Corporation, Tokyo, Japan
X-ray recording	Cesium iodide (CsI) phosphor + TFT array
Size	24 × 30 cm^2
Weight	1.5 kg
Matrix	1.536 × 1.920 pixel
Detector element size	150 µm
Detective quantum efficiency (DQE)	62 % (at 0 lp mm^{-1}, 1 mR) 54 % (at 1 lp mm^{-1}, 1 mR)
Modulation transfer function (MTF)	80 % (at 1 lp mm^{-1}, 1 mR)

and afterword each pixel is readout individually by the TFT. The amount of charge on a pixel is proportional to the incident radiation.

- Direct flat-panel detectors convert incident X-ray photons directly into electric charge. The detector has a photoconductor layer (e.g., amorphous selenium, a-Se) in lieu of the scintillator and the photodiode. An electric field is applied to this selenium layer. Underneath this selenium layer, a layer of electrodes transmit the released electrons to an array of TFTs. In this second layer, the electrons move perpendicular to the surface of the selenium layer and in the direction of the electric field. Afterwards, the TFTs sample and store the energy of the electrons for the readout process. The read-out process is similar to those of indirect flat-panel detectors.

All technologies have advantages and disadvantages with respect to handling and image quality [6]. Due to decreasing purchase and maintenance costs, and increasingly slimmer design, flat-panel radiography is on course to surpass use of computed radiography in veterinary medicine.

From a dose management point of view, ‘detector quantum efficiency’ (DQE) is certainly the most important parameter to characterize the detector performance [16]. DQE describes how efficient a detector is able to convert incoming X-rays into image information. An ideal detector is one that outputs the same signal to noise ratio (SNR) at it receives as input, has a DQE of 100 %. The DQE of any real detector is always below 100%. While comparing detectors with low and high DQE images from a detector with high DQE have a superior image quality because images have lower noise or, in other words, a higher SNR. Further, systems with higher DQE needs less detector entrance dose to achieve the same noise level than a system with lower DQE. A greater dose saving potential exists with those systems [6] (Table 3).

3. Development and Use of Exposure Tables

Exposure charts contain validated exposure settings for a given body region and radiographic projection, based in the main on the tissue thickness, while as many other variables as possible are standardized. In SFR they are needed to hit the narrow detector entrance dose limits to achieve constantly suitable film blackening and to thus avoiding image retakes (Fig. 1). In digital radiography of humans, exposure charts are applied to keep the detector entrance dose within predefined limits [29,35].

The idea behind the second part of this review is to demonstrate the principal approach to motivate users to establish their own exposure controlling system in a comparable manner. Recently, our institution replaced an older CR-system with a flat-panel system (Table 4). Due to the numerous necessary technical adjustments, the previous exposure tables were not adaptable. Completely new tables had to be developed and subsequently validated. As in a cookbook, the steps to construct exposure table - in this case, radiographs of the distal limb - should serve as an example and should prevent pitfalls.

3.1. Step 1 - Preparation

3.1.1. Definition of the Target Value the System-Specific Exposure Indicator and its Tolerable Range

The exposure index of the system is used to monitor the level of the detector entrance dose in an exposure series of phantoms. According to the manufacturer’s recommendations for the use of the detector in human radiology the target S-value and the tolerable range were set with 400 ± 10 % (Table 5).

3.1.2. Definition of the ‘Constant’ Parameters

Parameters that kept constant were: the X-ray machine (Super 100 CP, Philips Healthcare, Hamburg, Germany) with a 100 kW high-frequency generator; the focal spot size of 1.2 × 1.2 mm^2; focus to detector distance (FDD) of 100 cm; total filtration of 2.0 mm Al; and no antiscatter grid usage (Table 5). Uniform processing was employed for the individual projections. The parameters of the manufacturer’s multifrequency processing algorithms (APL Software V12.1, Fujifilm, Tokyo, Japan) had been optimized in previous studies.

3.1.3. Selection and Preparation of Phantoms

Cadaver limbs of three horses, representing three categories of patient size were used. These size categories were termed ‘Pony type’ (body weight of about 200 kg), ‘Warmblood type’ (body weight of about 450 kg) and ‘Noriker type’ (body weight of about 600 kg). For the radiographic studies, special fixation devices for the cadaver limbs and positioning devices for the detector were used (Fig. 5). In this way, standardized exposure conditions were given and radiation exposures of the people who carried out the examination could be avoided.

3.1.4. Designing Table Layout

The exposure table provides an overview about the variable conditions that has to be considered when selecting appropriate exposure settings: in particular body region, projection and patient thickness. To prevent mistakes for future users, the aforementioned ‘constant’ parameter should be visible on the chart. The provided example for the table layout design is based on 2 cm increments of patient thickness (Table 5). We recommend printing out the empty table and using a pencil and an eraser to enter and remove, as necessary, the settings identified.

3.2. Step 2 - Trial and Error

In the second step, image series with changing exposure parameters were taken of the fresh cadaver limbs to achieve the targeted EI range. An essential prerequisite is to measure the tissue thickness in the direction of the X-ray beam with a calliper. These measurements were performed at the limb level with the greatest thickness relative to the studied region and projection. Images were repeated to verify the reproducibility of the S-value. To prevent motion related unsharpness in living horses, the exposure time should not exceed 20 ms.

The setting (kVp - mAs combinations) identified in this way for the three size categories serves as landmarks while constructing the exposure table. Subsequently, exposure settings for remaining thicknesses of the respective body region are calculated by use of a simple exposure adaptation scheme (Fig. 6). It should be noted, that a number of alternative adaption methods for adding missing settings exists [36].

Table 5
Exposure table for radiographs of the distal limb of horses. The table is based on standardization of as many different parameters as possible. Variable parameters influencing S-value were tissue thickness and field size.

Region		Thickness (cm)							
Field size	Projection	6–7	8–9	10–11	12–13	14–15	16–17	18–19	20–21
	Carpus								
	dorso-palmar		60–2.5*		63–2.8′	66–3.0"			
	latero-medial		60–2.2*		63–2.5′"				
	oblique		60–2.5*		63–2.8′	66–3.0"			
	Metacarpal(tarsal) bone								
	dorso-palmar/plantar		60– 2.2*	60– 3.6'	63– 2.5"				
	latero-medial	60– 1.8*	60– 2.8'	60– 3.6"					
	oblique	60– 2.0*	60– 2.8'	60– 3.6"					
	Proximal - distal phalanx								
	dorso-palmar/plantar			60–3.2*		66–2.8'		72–4.0"	
	latero-medial		60–2.5*		63–2.5'		68–3.2"		
	Oblique		60–2.5*		63– 2.5'		68–3.2"		
	55°dorso-palmar/plantar (Oxspring)			60–2.8*		66– 2.8'	68– 3.2"		
	Tarsus								
	dorso-plantar			63– 2.8'			66– 5.6'		75– 8.0"
	latero-medial		60– 2.5*		63– 2.8'		68– 3.6"		
	oblique		60– 2.5*			66– 3.0'		72– 4.0 "	

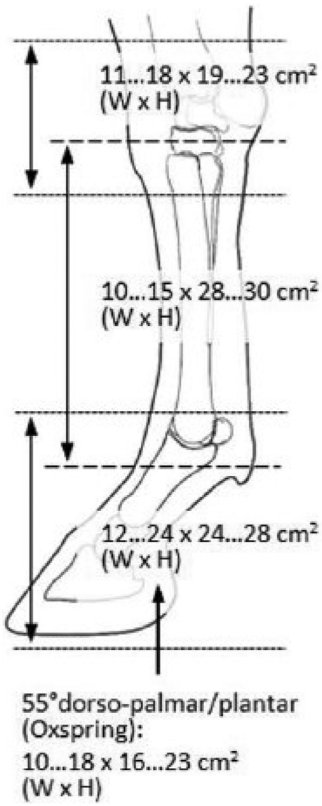

The recorded exposure settings (kVp - mAs combinations) for the target S-value of 400 (± 10 %) originate from test exposures of the cadaver limbs of three horses of different size (*Pony type, ‘Warmblood type, “Noriker type). Subsequently, missing settings need to be adjusted by assigning each ± 1 cm tissue thickness difference to ± 1 exposure points (EP) difference. To determine open exposure settings, to the closest approved setting in the table the adequate number of EPs is added (or subtracted). The corresponding new mAs- or kVp-values (Fig. 6) are filled in the open boxes of the exposure table.

Because of the strong influence of collimation on the exposure indicator value, the borders of the collimation as determined by the light beam diaphragm are also documented in the table to ensure consistency in collimation (Table 5). Subsequent changes of the collimation are requiring additional exposure setting adjustments.

3.3. *Step 3 - Fine Tuning*

Once the table has been completed the predefined settings are monitored in clinical routine. The displayed exposure indicator value acts as control tool for the verification of the formerly recorded data (Fig. 3). If necessary, the setting needs to be corrected. Because of the afore described dependence of the exposure indicator from small differences in the tissue thickness, careful thickness measurements by use of a calliper are required. After validation of the data, they are transferred into the final version of the table and presented within the radiographic unit.

4. Current Status and Considerations for Future Adjustments

Unlike screen-film systems, in digital radiography, image brightness is not usable as an indicator for a correct choice of the exposure parameters. Therefore, alternative methods for detector entrance-dose surveillance needs to be implemented into the clinical routine. The primary aim of dose monitoring in human radiology is to keep the dose of human patients as low as possible whilst ensuring sufficient image quality. In veterinary digital radiology, the selection of appropriate exposure settings also plays an important role in radiation safety. However, in contrast with human radiology, radiation safety is focused on protecting assisting staff from avoidable radiation exposure.

The current philosophy of radiation protection is based on the assumption that without a threshold dose even small doses of ionizing radiation can - with correspondingly low probability - cause cancer or hereditary damage and that these stochastic radiation risks increase linearly with arising dose (‘Linear - No threshold Theory’, LNT) [37]. The systematic use of unjustified excessive detector entrance doses directly correlates with an increase of the effective doses of holding staff and of the animal patients. Especially when it is often the same, experienced persons who are carrying out the examinations, the dose accumulation might progress rapidly [38,39]. Purposeful overexposure to ‘be on the safe side’ is unacceptable and clearly violates the ALARA (‘as low as reasonably achievable’) principle [9].

We present a concept that makes it possible to firstly adjust the level of the detector entrance dose and subsequently monitor the generated exposure settings in routine clinical veterinary radiography.

In the proposed concept, the inherent system exposure indicator plays a central role. It is used for different purposes: as a benchmark for the detector entrance dose while identifying proper

Fig. 5. Experimental setting for image series of a cadaver limb. The detector, embedded in the cover box, is capable to store all the image of one series. Consequently, there was no need for any changes to the condition of admission. For a new image exclusively the mAs-settings had to be changed at the control panel.

exposure settings, in the subsequent monitoring of their appropriateness and - if necessary - for subsequent fine-tuning of the settings. Although the exposure indicator is not directly based on dose measurements, it has an overall good correlation to the detector entrance dose and - despite other influencing factors - is suitable for monitoring exposure settings [30].

Once the ideal exposure settings have been established on trial patients or phantoms, simple mathematical relationships can be used to fill in the table for any other thickness of the corresponding body region. This table is a working chart and needs to be tested on a variety of animals. With resulting minor corrections, ultimately the table becomes a reliable practical tool.

The constructed exposure tables are based on tissue-thickness measurements. In our study we could confirm that even small differences in tissue thickness require adjustments of the exposure settings: an increase of tissue thickness of 3 cm requires an approximate doubling of the detector entrance dose [36]. Neither the body weight of the patient nor the use of animal size groups can serve as resilient fundaments for the establishment of exposure tables because of their poor correlation with tissue thickness. Similar observations have been reported from examinations in pediatric radiology [35].

The absolute numbers in the presented exposure table are not intended for use verbatim. Except patient related factors (e.g., body region, projection, thickness) deviating equipment and exposure conditions - such as DQE of the detector, output of generator, capacity of the tube, additional beam filtration, focus - detector distance, collimation, and characteristics for the antiscatter grid (ratio, type, Bucky factor) - make the table values in general non-transferrable. However, for very similar conditions these might be adaptable.

mAs	kVp
40	1.00
41	1.25
42	1.60
44	2.00
46	2.50
48	3.20
50	4.00
52	5.00
55	6.40
57	8.00
60	10.00
63	12.50
66	16.00
70	20.00
73	25.00
77	32.00
81	40.00
85	50.00
...	...

Fig. 6. Exposure adaptation scheme. The steps from value to value within the two columns for mAs, respectively kVp, are equivalent to 1 exposure point ('EP') (± 1 EP = ± 1 cm tissue thickness). Changes in the mAs value are linearly related to the detector dose: a doubling of the detector dose, which becomes necessary when the thickness increases by 3 cm, requires doubling of mAs. Differently, the kVp-value is not linearly related with the detector dose: at low kVp, changes in kVp have a much stronger effect on the detector dose than at high kVp-values. At low kVp (40–50 kVp) the exponent is around five and at high kVp (120–150 kVp) the exponent is around three (adapted from [52]).

The constructed table can further serve as a starting point for dose reduction testing. In image quality studies - in the simplest case by means of visual subjective assessment - it can be checked whether a dose reduction is possible basically throughout all regions and projections or whether this only might only be possible for specific predefined indication where a lower SNR is tolerable (e.g., follow-up control post osteosyntheses) [7]. In human radiology, concepts with three image-quality classes (high, medium, low) are proposed. The dose is halved from class to class [19,40,41]. The introduction of comparable image quality classes into the veterinary radiology routine would involve considerable changes in work processes, because the required image quality class must be selected prospectively before each examination. Drawing on our experience, this is unlikely be feasible for many examinations. A realistic scenario for a significant dose reduction is given for detectors with high DQE [7,42].

Medical imaging examinations should use acquisition techniques that are repeatable and adjusted to administer the lowest radiation dose that yields a diagnostic image quality. As demonstrated, the linear course of the 'characteristic curve' makes it necessary to find the right balance between the needs of dose discipline and the safeguarding of a diagnostic image quality [14,43]. In this interrelationship, dose requirements acts as determinant. For radiation safety reasons, a predefined level of dose must not be exceeded. As a target for this aimed level, detector entrance doses formerly used in SFR for otherwise identical exposure conditions could be taken as a landmark.

For generating a maximum of image quality at a given level of detector entrance dose, it is necessary that every single element of the imaging chain (signal recording, signal processing, image display) are of high performance and the links are well matched up. The weakest element in this chain ultimately determines the quality of the image and thus its diagnostic suitability [19,42,44,45]. Image processing has a considerable influence on the visual perception of image noise and on other parameters characterizing image quality. Studies in human radiology have shown that with conventional processing software (e.g., Unsharp mask filtering and variants of it), the application of edge-enhancing parameters improves detail perception, but also emphasize noise [46]. In other studies with conventional software, the application of optimized processing parameters partially compensated noise sensation. This was more effective at low detector entrance doses than at higher dose levels [7,47]. New developments in processing algorithms, based on multifrequency software tools, allow suppression of noise and the improvement of image detail rendition at the same time [47,48]. In an image quality study with images of the proximal ovine hind limb, it was shown that due to the optimization of the multifrequency processing software, a reduction of the detector entrance dose of up to 61% can be achieved without loss of image information, as compared to reference images. Even for images of diagnostically acceptable quality, adapted processing supported a dose reduction of 88%. Accordingly, the corresponding effective dose was reduced from 79 μSv to 4 μSv [49]. Specific veterinary studies focused on the influences of processing onto image quality are rare [50,51]. Considering the similar requirements for the presentation of image details, it can be assumed that there is also considerable potential for dose reduction in veterinary radiography. Therefore, we recommend that the veterinary user in cooperation with an expert of the manufacturer or vendor should optimize parameters of image processing software with respect to the diagnostic requirements of image quality and to the detector entrance dose.

5. Conclusions

In summary, keeping exposures as low as reasonably achievable and monitoring exposure to radiation are key elements of practical radiation safety. Digital radiographic examinations should use techniques that are adjusted to use the lowest detector entrance dose that yields diagnostic image quality. A robust and easily applicable method to ensure a constant diagnostic image quality and thereby keeping control over the exposure level is to utilize exposure tables for respective body regions and projections on the basis of tissue thickness measurements. The system-specific exposure indicator is - despite the number of influences other than exposure settings on it - a reliable monitoring tool for: (1) constructing exposure tables; (2) exposure monitoring during routine clinical radiography and; (3) the evaluation of dose saving potentials.

It is recommended that purchasing DRx with high DQE, offers substantial higher potentials for image quality or dose saving. Furthermore, adjustments of processing algorithms have been proven to be an important factor in achieving best image qualities. Optimized the processing parameters can therefore compensate/maintain image quality while the user benefits from the reduced risk a decreased dose brings.

Disclaimer

Mention of trade names or commercial products in the article is solely for the purpose of providing specific information and does not imply recommendation or endorsement.

References

[1] Booth NJ, Morley SJ, Ewers RS. Use of radiography in small animal practice in the UK and Republic of Ireland in 2013. Vet Rec 2018;182:225.
[2] Skelly C. Comparative studies in veterinary radiography in Ireland. PhD thesis. Ireland: University College Dublin; 2014.
[3] McKnight A. Digital radiography in equine practice. Clin Tech Equine Pract 2004;4:352–60.
[4] Nelson NC, Zekas LJ, Reese DJ. Digital radiography for the equine practitioner: basic principles and recent advances. Vet Clin North Am Equine Pract 2012;28:483–95.
[5] Ludewig E, McEvoy FJ. Basics of musculoskeletal radiography and radiology. In: Kirberger RM, McEvoy FJ, editors. BSAVA manual of canine and feline musculoskeletal imaging. Gloucester: British Small Animal Veterinary Association; 2016. p. 1–14.
[6] Seeram E. Digital radiography - physical principles and quality control. Singapore: Springer; 2019.
[7] Knight SP. Contemporary research in digital radiography. J Med Radiat Sci 2020;67:254–6.
[8] Mattoon JS. Digital radiography. Vet Comp Orthop Traumatol 2006;19:123–32.
[9] International Atomic Energy Agency (IAEA) Radiation protection and safety in veterinary medicine, Vienna: IAEA; 2021. Safety Report Series No. 104.
[10] Bansal GJ. Digital radiography. A comparison with modern conventional imaging. Postgrad Med J 2006;82:425–8.
[11] Körner M, Weber CH, Wirt S, Pfeifer KJ, Reiser MF, Treitl M. Advances in digital radiography: physical principles and system overview. Radio Graphics 2007;27:675–86.
[12] Ritenour ER. Physics overview of screen-film radiography. Radio Graphics 1996;16:903–16.
[13] Drost WT, Reese DJ, Hornof WJ. Digital radiography artifacts. Vet Radiol Ultrasound 2008;49:S48–56.
[14] Dixon J, Biggi M, Weller R. Common artefacts and pitfalls in equine computed and digital radiography and how to avoid them. Equine Vet Educ 2018;30:326–35.
[15] Vano E, Fernandez JM, Ten JI, Prieto C, Gonzalez L, Rodriguez R, de Las Heras H. Transition from screen-film to digital radiography: evolution of patient radiation doses at projection radiography. Radiology 2007;243:461–6.
[16] Lanca L, Silva A. Digital radiography detectors - a technical overview: part 2. Radiography 2009;15:134–8.
[17] Busch HP, Busch S, Decker C, Schilz C. Bildqualität und Dosis in der digitalen Projektionsradiographie. Fortschr Röntgenstr 2003;175:32–7.
[18] Ludewig E, Pees M, Morgan JP. Clinical technique: digital radiography in exotic pets - important practical differences compared with traditional radiography. J Exot Pet Med 2012;21:71–9.
[19] Uffmann M, Schaefer-Prokop C, Neitzel U. Abwägung von Dosisbedarf und Bildqualität in der digitalen Radiographie. Radiologe 2008;48:249–57.
[20] Willis CE, Slovis TL. The ALARA concept in pediatric CR and DR: dose reduction in pediatric radiographic exams - a white paper conference executive summary. Pediatr Radiol 2004;34:S162–4.
[21] Gibson DJ, Davidson RA. Exposure creep in computed radiography: a longitudinal study. Acad Radiol 2012;19:458–62.
[22] Mothiram U, Brennan PC, Robinson J, Lewis SJ, Moran B. Retrospective evaluation of exposure index (EI) values from plain radiographs reveal important considerations for quality improvement. J Med Radiat Sci 2013;60:115–22.
[23] Seibert JA, Morin RL. The standardized exposure index for digital radiography: an opportunity for optimization of radiation dose to the pediatric population. Pediatr Radiol 2011;41:573–81.
[24] International Atomic Energy Agency (IAEA) Avoidance of unnecessary dose to patients while transitioning from analogue to digital radiology, Vienna: IAEA; 2011. IAEA-TECDOC-1667.
[25] Takaki T, Takeda K, Murakami S, Ogawa H, Ogawa M, Sakamoto M. Evaluation of the effects of subject thickness on the exposure index in digital radiography. Radiol Phys Technol 2016;9:116–20.
[26] Baker M. Investigation into factors influencing Fuji S-value using an extremity phantom. J Med Imag Radiat Sci 2012;43:34–7.
[27] International Electrotechnical Commission (IEC) Medical electrical equipment: exposure index of digital x-ray imaging systems. Part 1. Definitions and requirements for general radiography, Geneva: IEC; 2008. International standard IEC 62494-1.
[28] Shepard SJ, Wang J, Flynn M, Gingold E, Goldman L, Krugh K, Leong DL, Mah E, Ogden K, Peck D, Samei E, Wang J, Willis CE. An exposure indicator for digital radiography: AAPM Task Group 116 executive summary. Med Phys 2009;36:2898–914.
[29] Scott AW, Zhou Y, Allahverdian J, Nute JL, Lee C. Evaluation of digital radiography practice using exposure index tracking. J Appl Clin Med Phys 2016;17:343–55.

[30] Dave JK, Jones AK, Fisher R, Hulme K, Rill L, Zamora D, Woodward A, Brady S, MacDougall RD, Goldman L, Lang S, Peck D, Shepard SJ, Uzenoff R, Willis C. Current state of practice regarding digital radiography exposure indicators and deviation indices: report of AAPM Imaging Physics Committee Task Group 232. Med Phys 2018;45:e1146–60.
[31] Don S, Whiting BR, Rutz LJ, Apgar BK. New exposure indicators for digital radiography simplified for radiologists and technologists. Amer J Radiol 2012;199:1337–41.
[32] Erenstein HG, Browne D, Curtin S, Dwyer RS, Higgins RN, Hommel SF, Menzinga J, Pires Jorge JA, Sauty M, de Vries G, England A. The validity and reliability of the exposure index as a metric for estimating the radiation dose to the patient. Radiography 2020;26:S94–9.
[33] Neitzel U. Status and prospects of digital detector technology for CR and DR. Radiat Prot Dosimetry 2005;114:32–8.
[34] Lanca L, Silva A. Digital radiography detectors - a technical overview: part 1. Radiography 2009;15:58–62.
[35] Knight SP. A paediatric X-ray exposure chart. J Med Radiat Sci 2014;61:191–201.
[36] Ching W, Robinson J, McEntee M. Patient-based radiographic exposure factor selection: a systematic review. J Med Radiat Sci 2014;61:176–90.
[37] Kellerer AM. Risk estimates for radiation-induced cancer – the epidemiological evidence. Radiat Environ Biophys 2000;39:17–24.
[38] Busse C. Untersuchungen zur Strahlenexposition von Tierhaltern und Hilfspersonal bei radiographischen Standardverfahren in der Klinik für Pferde (Investigation of radiation exposure of horse owner and staff during standard X-ray examinations in the Clinic for Horses). Doctoral thesis. Germany: University of Veterinary Medicine Hanover; 2008.
[39] Ludewig E, Gensler A, Oechtering G, Gosch D. Ergebnisse dosimetrischer Untersuchungen in der Kleintierpraxis: welchen Einfluss haben der Abstand und die Position des Untersuchers zum Patienten? Berl Münch Tierärztl Wochenschr 2010;123:506–15.
[40] Busch HP, Faulkner K. Image quality and dose management in digital radiography: a new paradigm for optimization. Radiat Prot Dosimetry 2005;117:143–7.
[41] Vano E. ICRP recommendations on "managing patient dose in digital radiology. Radiat Prot Dosimetry 2005;114:126–30.
[42] Bath M. Evaluating imaging systems: practical applications. Radiat Prot Dosimetry 2010;139:26–36.
[43] Uffmann M, Schaefer-Prokop C. Digital radiography: the balance between image quality and required radiation dose. Eur J Radiol 2009;72:202–8.
[44] Bath M, Hakansson M, Hansson J, Mansson LG. A conceptual optimisation strategy for radiography in a digital enivironment. Radiat Prot Dosimetry 2005;114:230–5.
[45] Redlich U, Hoeschen C, Effenberg O, Fessel A, Preuß H, Reißberg S, Scherlach C, Döhring W. Vergleich von vier digitalen und einem konventionellen Röntgenaufnahmesystem für den Thorax mittels einer Patientenstudie mit nachfolgender Systemoptimierung. Fortschr Röntgenstr 2005;177:272–8.
[46] Redlich U, Hoeschen C, Doehring W. Assessment and optimisation of the image quality of chest-radiography systems. Radiat Prot Dosimetry 2005;114:264–8.
[47] Prokop M, Neitzel U, Schaefer-Prokop C. Principles of image processing in digital chest radiography. J Thorac Imaging 2003;18:148–64.
[48] Schaefer-Prokop C, Eisenhuber E, Fuchsjäger M, Puig S, Prokop M. Aktuelle Entwicklungen auf dem Gebiet der digitalen Thoraxradiographie. Radiologe 2001;41:230–9.
[49] Precht H, Gerke O, Rosendahl K, Tingberg A, Waaler D. Digital radiography: optimization of image quality and dose using multi-frequency software. Pediatr Radiol 2012;42:1112–18.
[50] Lo WY, Hornof WJ, Zwingenberger AL, Robertson ID. Multiscale image processing and antiscatter grids in digital radiography. Vet Radiol Ultrasound 2009;50:569–76.
[51] Shimbo G, Tagawa M, Matsumoto K, Tomihari M, Miyahara K. Effects of scatter correction processing on image quality of portable thoracic radiography in calves. Jpn J Vet Res 2018;66:105–12.
[52] Hölzemann H. Das Belichtungspunktesystem und seine Bedeutung in der digitalen Radiographie (Teil 2) 2015 [Internet] MTA Dialog, Deutscher Ärzteverlag; https://www.mta-dialog.de/artikel/das-belichtungspunktesystem-und-seine-bedeutung-in-der-digitalen-radiographie-teil-2 [accessed 09.01.2022]).
[53] Neitzel U. The exposure index and its standardization 2006 [Internet]. Philips Medical Systems, Hamburg, Germany; https://silo.tips/download/the-exposure-index-and-its-standardization [accessed 09.01.2022]).